Thin Solid Films 519 (2011) 5875–5881

Contents lists available at ScienceDirect

Thin Solid Films

journal homepage: www.elsevier.com/locate/tsf

Polarity of heavily doped ZnO films grown on sapphire and SiO_2 glass substrates by pulsed laser deposition

Yutaka Adachi [a,*], Naoki Ohashi [a,b,f], Takeshi Ohgaki [c], Tsuyoshi Ohnishi [b], Isao Sakaguchi [a], Shigenori Ueda [d], Hideki Yoshikawa [d], Keisuke Kobayashi [d], Jesse R. Williams [e], Tsuyoshi Ogino [f], Hajime Haneda [c,f]

[a] Optronic Materials Center, National Institute for Materials Science (NIMS), 1-1 Namiki, Tsukuba, Ibaraki 305-0044, Japan
[b] International Center for Materials Nanoarchitectonics (MANA), NIMS, 1-1 Namiki, Tsukuba, Ibaraki 305-0044, Japan
[c] Sensor Materials Center, NIMS, 1-1 Namiki, Tsukuba, Ibaraki 305-0044, Japan
[d] NIMS Beamline station at SPring-8, NIMS, 1-1-1 Kouto, Sayo-cho, Sayogun, Hyogo 679-5148, Japan
[e] International Center for Young Scientists (ICYS), MANA, NIMS, 1-1 Namiki, Tsukuba, Ibaraki 305-0044, Japan
[f] Department of Applied Science for Electronics and Materials, Kyushu University, 6-1 Kasuga Koen, Kasuga, Fukuoka 816-8580, Japan

ARTICLE INFO

Article history:
Received 2 August 2010
Received in revised form 23 February 2011
Accepted 23 February 2011
Available online 11 March 2011

Keywords:
Zinc oxide
Glass substrate
Crystalline polarity
Hard X-ray photoelectron spectroscopy
Doping

ABSTRACT

The crystalline polarity of undoped and impurity-doped ZnO films grown on SiO_2 glass substrates was investigated with the goal of achieving polarity-selective growth of ZnO films on non-crystalline substrates. We first demonstrated that hard X-ray photoelectron spectroscopy (HX-PES) is an appropriate method for determining the crystalline polarity of ZnO. We then characterized the ZnO films grown by pulsed laser deposition using HX-PES. The resulting films deposited with a 1 mol% Al-doped ZnO target had the (0001) surface, whereas films grown with nominally undoped, 0.1 mol% Al-doped, 1 mol% Ga-doped, and 1 mol% In-doped ZnO targets had the $(000\bar{1})$ surface. Since a clear polarity change due to Al-doping was seen at the ZnO/glass structure, we conclude that the essential parameter governing the polarity of the ZnO films is unlikely lattice matching (alignment of the lattice on the atomic scale) at the heterointerface between the ZnO films and substrates.

© 2011 Elsevier B.V. All rights reserved.

1. Introduction

ZnO has received a great deal of attention due to the wide range of its technological applications. The high optical transparency of ZnO in the visible range along with good electrical conductivity makes it suitable for application as transparent electrodes in flat panel displays and solar cells [1,2]. ZnO-based heterostructures have been extensively investigated for applications in optoelectronic devices such as ultraviolet light emitting diodes (LEDs) [3,4] and transparent field-effect transistors [5,6].

A ZnO crystal has a wurtzite-type structure; hence, it shows spontaneous electrical polarization along the c-axis and thereby has polar surfaces corresponding to the $(000\bar{1})$ face (c(−)-face) and (0001) face (c(+)-face). Furthermore, various properties of ZnO depend on its polarity, including the surface electronic structure [7], chemical stability of the surface [8], interfacial properties [9], and impurity incorporation [10]. Therefore, when designing devices using ZnO, it is important to understand the effects governing the crystalline polarity of ZnO and to develop a crystal growth technology to enable the polarity-selective growth of ZnO films. It has been previously reported that a ZnMgO/ZnO heterostructure with the $(000\bar{1})$ face is more suitable for high electron mobility transistor devices than the heterostructure with the (0001) face [11].

There have been several reports on the surface polarity of ZnO films deposited on sapphire substrates [12–17]. Nominally undoped ZnO films grown on a (0001) sapphire substrate tend to have the $(000\bar{1})$ face [12], and growth of ZnO with the (0001) face on native (0001) sapphire substrates is difficult. To overcome this tendency, the use of a buffer layer has been considered, and deposition of ZnO with the (0001) face on a sapphire substrate has been achieved by inserting thin epitaxial buffer layers of MgO [13], AlN [14], GaN [15], or Cr compounds [16] between the ZnO film and the sapphire substrate. The growth of undoped ZnO films with the (0001) face on native (0001) sapphire substrates has been reported only for film deposition by pulsed laser deposition (PLD) using very specific growth conditions: low growth temperatures (450 °C) with high growth rate on an atomically flat sapphire substrate [17]. These previous studies show that the polarity-selective growth of ZnO on crystalline substrates is possible if very specific growth conditions are used or when a buffer layer is applied. In contrast, polarity-selective growth of ZnO on a non-crystalline substrate has not yet been established, even though the deposition of ZnO on glass substrates is of great importance for industrial applications. Thus, it is crucial that a polarity control technique for ZnO on non-crystalline substrates, such as glass, be developed.

* Corresponding author. Tel.: +81 29 860 4438; fax: +81 29 855 1196.
E-mail address: adachi.yutaka@nims.go.jp (Y. Adachi).

0040-6090/$ – see front matter © 2011 Elsevier B.V. All rights reserved.
doi:10.1016/j.tsf.2011.02.087

Recently, we reported that Al-doping into ZnO led to the inversion of polarity of ZnO films on sapphire substrates [18]. Nominally undoped ZnO films grown by PLD have the $(000\bar{1})$ face, as mentioned above, whereas films prepared by PLD using a heavily (1 mol%) Al-doped ZnO target have the (0001) face. This polarity change of PLD-grown ZnO films by using a heavily Al-doped target was observed regardless of the substrate orientation. In fact, ZnO films with the $(000\bar{1})$ face could be deposited not only on (0001) sapphire substrates but also on $(11\bar{2}0)$ sapphire one by using the heavily Al-doped target [18]. These results suggest that the atomic arrangement at a substrate surface is not a major factor for determining the polarity of growing ZnO films, because the atomic configuration at the (0001) sapphire surface is considerably different from that at the $(11\bar{2}0)$ surface. Thus, we speculated that the polarity change induced by Al-doping was a macroscopic phenomenon, and this effect was insensitive to the substrate material. We were therefore motivated to examine the effects of Al-doping on the crystalline polarity of ZnO grown on a non-crystalline substrate such as glass.

For investigating the polarity of ZnO films on glass substrates, we also need to develop a methodology for determining the crystalline polarity of ZnO films with distinct in-plane rotation domains. For instance, ZnO on a non-crystalline substrate shows random orientation of the a-axis, though it is grown along the c-axis. Previously, determining the polarity of ZnO has been carried out using coaxial impact collision ion scattering spectroscopy (CAICISS) [12], convergent beam electron diffraction (CBED) [19], scanning probe microscopy [20], etching by acid [21], and X-ray diffraction using anomalous dispersion [22]. These techniques however have very specific requirements for polarity determination. For example, CAICISS requires a single crystalline sample with sufficient dimensions; CBED requires sufficiently larger grain size than the probe size as well as accurate sample thickness determination and high sample quality. Recently, we found that hard X-ray photoelectron spectroscopy (HX-PES) [23] is also appropriate for determining the crystalline polarity of ZnO [24]. In fact, the spectral profile of ZnO, particularly that in the valence band region, shows strong dependence on the crystalline polarity.

The work presented in this paper examined undoped and heavily doped ZnO films deposited on silica (SiO_2) glass substrates. The films obtained were characterized by HX-PES to reveal the effects of Al-doping on the polarity of ZnO films on non-crystalline substrates. We found that the PLD-grown ZnO films had the (0001) face regardless of the substrate materials when heavily doped with Al, whereas the PLD-grown undoped ZnO films tended to have the $(000\bar{1})$ face. Also, the effects of Ga- and In-doping into ZnO on film polarity were investigated. In our previous paper [18], we only reported the results for 1 mol% Al-doped ZnO films. It is well known that Ga and In act as a donor as well as does Al. It is also important for device applications of ZnO to investigate whether Ga- or In-doping results in a polarity change. In addition, we also studied the polarity of undoped ZnO film with a few-monolayer-thick Al-doped ZnO buffer layer on a sapphire substrate to clarify where polarity inversion occurred. If the growth of the film with the (0001) face starts at the film/substrate interface, the multilayer film should show the (0001) face. Using these data, we discuss a possible mechanism for the observed polarity change due to impurity-doping.

2. Experimental details

Deposition of the ZnO films was carried out by PLD using the fourth-harmonic generation of a neodymium-doped yttrium gallium garnet (YAG:Nd) laser ($\lambda = 266$ nm) with a pulse width of 5 ns, a repetition rate of 5 Hz, and an averaged fluence of about 1 J/cm^2. The growth rate of the films was 0.018 to 0.022 nm/pulse. The film thickness of each sample is shown in Table 1. The substrates used were SiO_2 glass and sapphire with a mirror-polished surface. The sapphire substrate had the $(11\bar{2}0)$ face, which is appropriate for obtaining ZnO films with high crystallinity [25]. The targets used for the PLD growth were nominally pure and doped ZnO ceramics prepared by an ordinary ceramics process. The doped films were grown with a 1 or 0.1 mol% Al-doped target, or a 1 mol% Ga- or In-doped target. It should be noted that the unintentional impurity level in the target was on the order of 10^{16} cm^{-3} or less, according to the results of secondary ion mass spectrometry analysis. The pressure in the growth chamber was kept at 2 mPa by introducing pure oxygen (O_2) gas, and the substrate temperature was kept at 700 °C. The growth process was monitored in situ using reflection high energy electron diffraction. We also examined the effect of a buffer layer by depositing a several-atom-thick doped layer prior to the deposition of undoped ZnO.

Table 1
Electron concentration (n) at room temperature, film thickness (t), FWHM of the ω-scan profile of the 0002 diffraction peak, substrate and chemical composition of typical ZnO films.

Substrate	Doping	t / nm	n / cm^{-3}	FWHM of 0002 / °
Sapphire	Undoped	400	9.6×10^{16}	0.16
Sapphire	Al : 0.1 mol%	170	1.3×10^{19}	0.46
Sapphire	Al : 1 mol%	410	3.2×10^{20}	0.64
Sapphire	Ga : 1 mol%	240	6.5×10^{19}	1.46
Sapphire	In : 1 mol%	510	1.3×10^{19}	1.67
SiO_2 glass	Undoped	460	1.8×10^{18}	1.15
SiO_2 glass	Al : 1 mol%	490	3.0×10^{20}	1.34

The crystallinity of the PLD-grown films was analyzed using X-ray diffraction (XRD) (PANalytical X'Pert Pro MRD) equipped with a hybrid 2-bounce asymmetric Ge (220) monochromator and a Cu Kα source. The morphology of the films was characterized using atomic force microscopy (AFM) (SII SPA400) operated in tapping mode. Si probes having a spring constant of 14 N/m (SII SI-DF20) were used at a resonance frequency of 144 kHz. The electrical resistivity (ρ) of the films was measured by the van der Pauw method using ohmic Al or In electrodes formed on the sample surface, and Hall measurement was performed under a magnetic field of 0.5 T for determining the electron concentration (n) and mobility (μ). The temperature dependencies of ρ, n, and μ were measured over the range 80–350 K.

The polarity of the films deposited on the sapphire substrates was determined using CAICISS and CBED. Since CAICISS is a method for observing atomic arrangements close to the top-most surface, CBED was used to observe the polarity of the film close to the film/substrate interface. The experimental procedure for CAICISS has been published elsewhere [12,26]. The CBED experiments and simulations were performed by NTT Advanced Technology, Ltd., Atsugi, Kanagawa, Japan. For reference, their corresponding literature can be found elsewhere [27]. A bulk ZnO single crystal with known polarity was used as a standard sample for CAICISS analyses.

HX-PES measurements were performed at the undulator beamline BL15XU of SPring-8. The X-ray photon energy was fixed at 5.95 keV, and spectra were obtained at room temperature using a VG Scienta R4000 electron energy analyzer. The total energy resolution was set to 250 meV, as verified with the Fermi cut-off of an evaporated Au thin film. The take-off angle (TOA) of the photoelectrons from the surface was set to 85–88° to perform bulk-sensitive measurements. This high TOA was used for determining the crystalline polarity of ZnO from the HX-PES spectra. The angle between the incident X-rays and the analyzer was fixed at 90°. Details of the experimental setup and procedures of the HX-PES measurements are described elsewhere [23,26,28–30].

3. Results

3.1. Structural and electrical properties of ZnO films on sapphire and glass substrates

All the films on the sapphire and glass substrates were grown along the c-axis. The films on the sapphire substrate showed six well-

defined poles within XRD pole-figure measurements, similar to our previous results [18], indicating that the a-axis of the films grown on the sapphire substrate was also well aligned in the in-plane direction. The films on the glass substrate were also grown along the c-axis but showed random in-plane orientation, and the peak width [full width at half maximum (FWHM)] of the ω-scan profile of the 0002 diffraction peak for the films on the glass substrate was relatively broad compared to the films on the sapphire substrate, as shown in Table 1. Surface morphology examined using AFM showed that Al-, In-, and Ga-doping reduced the grain size, and the use of the glass substrate also reduced the grain size compared to the sapphire substrate, as shown in Fig. 1. Thus, the small grain size of the films is one of the reasons for the relatively broad XRD peaks of the films.

The electron concentration (n) at room temperature was on the order of $10^{20}\,\mathrm{cm}^{-3}$ for the heavily Al-doped films deposited with the 1 mol% Al-doped target, whereas n for the undoped films was on the order of 10^{16} to $10^{18}\,\mathrm{cm}^{-3}$. Typical parameters obtained from Hall measurements are listed in Table 1. The n for the Al-doped film prepared with the 0.1 mol% Al-doped target was on the order of $10^{19}\,\mathrm{cm}^{-3}$. This result suggests that the added Al in the ZnO targets was incorporated into the ZnO lattice, causing a shallow donor state. In contrast to the Al-doped films, Ga-doped and In-doped films showed relatively less n (see Table 1). The lower carrier concentration is likely explained by a change in the local structure around the In and Ga impurities in ZnO. In fact, homologous series compounds of $(\mathrm{In,Ga})_2\mathrm{O}_3[\mathrm{ZnO}]_n$ are known to be thermally stable, whereas In and Ga in these homologous structures tend to be at octahedral rather than tetrahedral sites and do not act as donors [31]. Since the growth temperature used in this study was relatively high, the structure around Ga and In in ZnO may have been strained to form an octahedral structure. Further study is needed to explain why n was comparatively low in the Ga- and In-doped ZnO films prepared in this study.

3.2. Polarity of ZnO films on sapphire substrates

Fig. 2 shows typical CAICISS spectra for the films deposited on the sapphire substrate. The undoped film (n on the order of $10^{16}\,\mathrm{cm}^{-3}$) yielded a CAICISS profile similar to that from the $(000\bar{1})$ face of a bulk single crystal. In contrast, the heavily Al-doped film (n on the order of $10^{20}\,\mathrm{cm}^{-3}$) exhibited a CAICISS profile similar to that for the (0001) face. This means that the nominally undoped film on the sapphire substrate had the $(000\bar{1})$ surface but the heavily Al-doped film had the (0001) surface. This result was consistent with the previous study on the undoped films [12] and our previous study on the Al-doped films [18]. The CAICISS profile for the Ga-doped films showed an intermediate structure between that of the (0001) and $(000\bar{1})$ face of

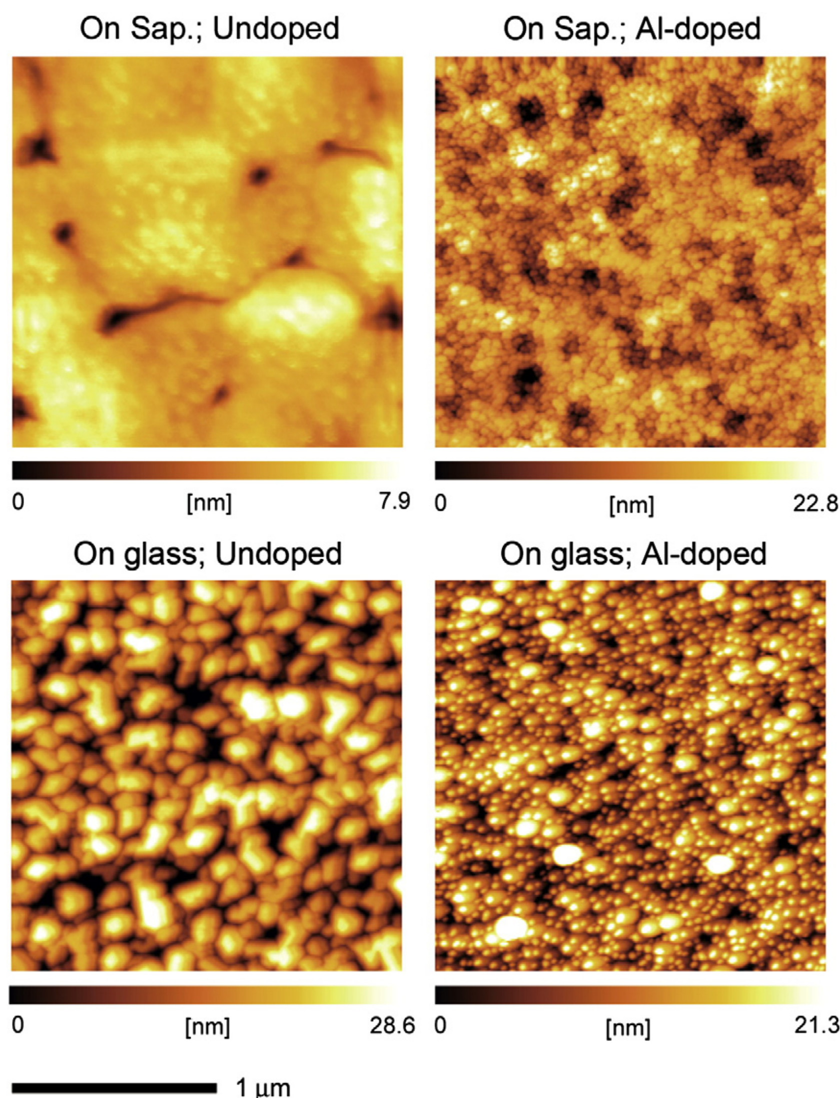

Fig. 1. Typical AFM images of the undoped and doped ZnO films deposited on sapphire (Sap.) and glass substrates. Height scales are given for each image and the length scale is common to all the images.

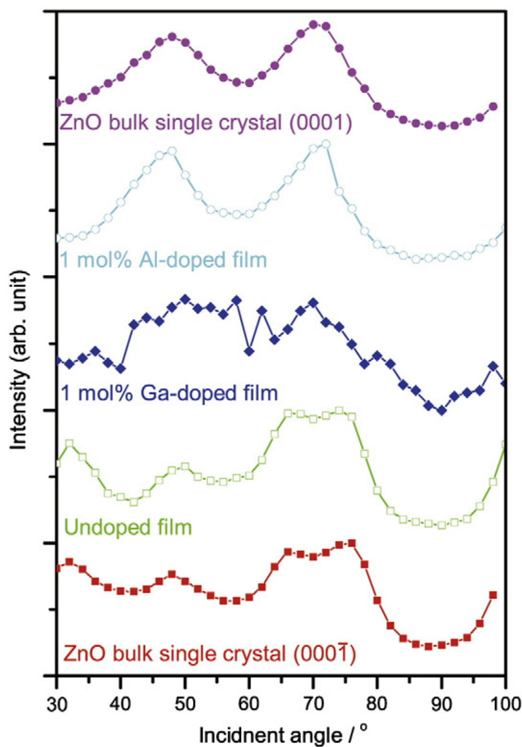

Fig. 2. Typical CAICISS spectra of the doped and undoped ZnO films on sapphire substrates compared to those of bulk ZnO single crystals. (See text and reference for the CAICISS technique).

the bulk ZnO crystal, indicating that the Ga-doped film had a multi-domain structure composed of grains with the (0001) and (000$\bar{1}$) surfaces. These CAICISS results show that the clear polarity change due to the doping was only seen in the heavily Al-doped films.

Fig. 3 shows the CBED patterns obtained from three different regions in the undoped films and from the surface region of the heavily Al-doped (n on the order of 10^{20} cm^{-3}) films on the sapphire substrate. The regions analyzed using CBED are shown by circles in the transmission electron microscope (TEM) images in the figure. Since the grain size of the Al-doped film was much smaller than that in the undoped film, the CBED pattern of the Al-doped film could only be obtained from the surface region, where the size of the ZnO columnar grains was larger than the electron probe, and there was no overlap of the columns along the probe path. The polarity at the observed region was determined by comparing the observed CBED patterns with simulated ones. All three regions in the undoped film had the same polarity, with the (0001) face at the film/substrate interface and the (000$\bar{1}$) face at the surface, whereas the polarity in the heavily Al-doped film was opposite, with the (0001) face at the surface and the (000$\bar{1}$) face at the film/substrate interface. Thus, the results of CAICESS and CBED analyses were consistent with each other, and it was confirmed that the undoped (n on the order of 10^{16} cm^{-3}) and heavily Al-doped (n on the order of 10^{20} cm^{-3}) films on the sapphire substrate had the (000$\bar{1}$) surface and the (0001) surface, respectively.

Fig. 4 shows the valence band HX-PES spectra of the ZnO films grown on the sapphire substrate compared to those of ZnO bulk single crystals. The spectral profile for the (0001) and (000$\bar{1}$) faces of the bulk crystal differed by a characteristic structure locating at a binding energy (E_B) of 5 eV, as found in our previous study [23]. As shown by the arrows in Fig. 4, a sub-peak was visible in the HX-PES profile for the (0001) face but was not observed in the HX-PES profile for the (000$\bar{1}$)

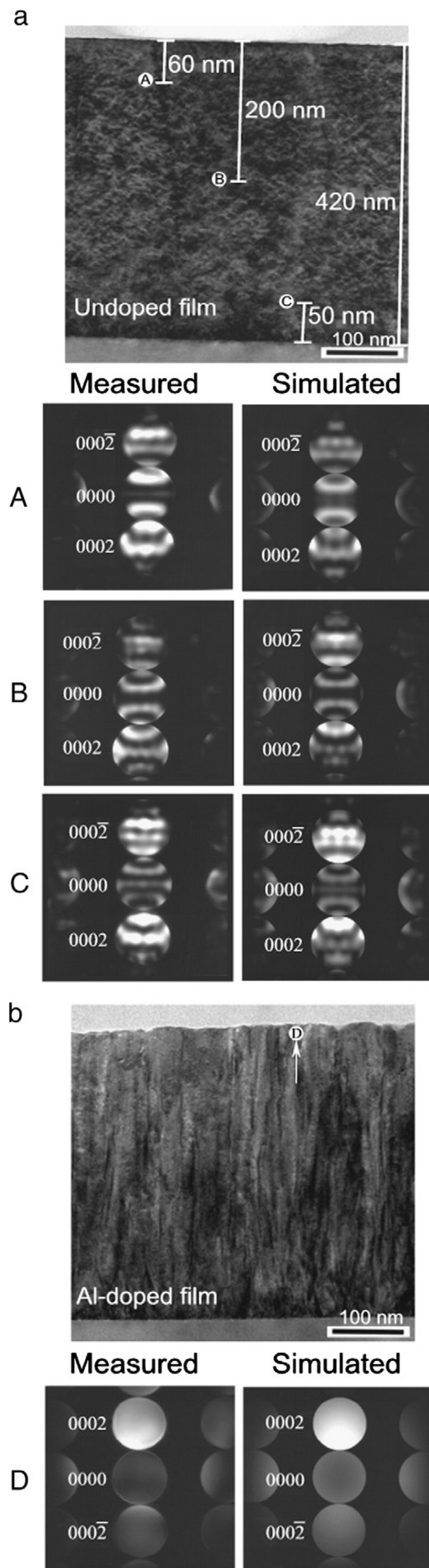

Fig. 3. TEM images and CBED patterns of (a) undoped and (b) Al-doped films on the (11$\bar{2}$0) face of sapphire. The circles in the TEM images indicate the region analyzed using CBED. (See text and reference for the CBED technique).

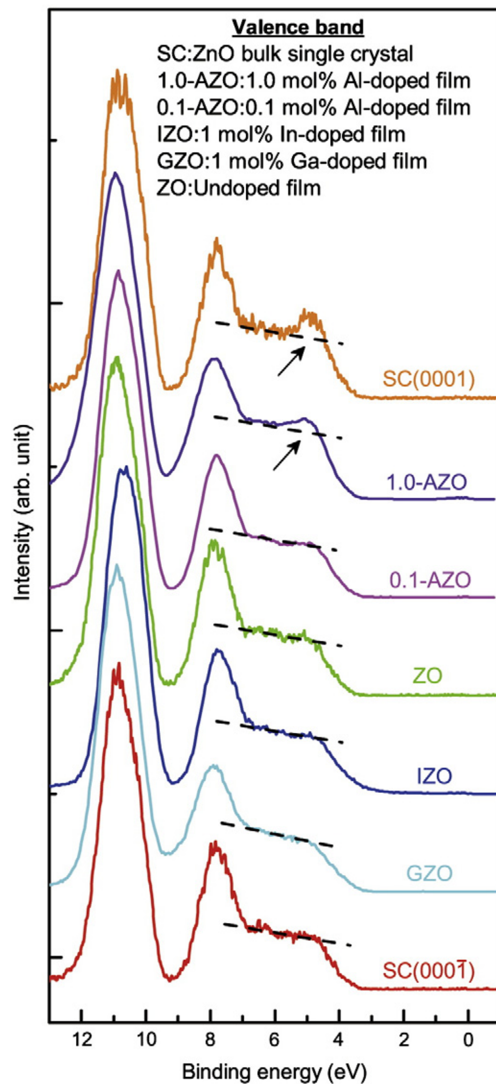

Fig. 4. HX-PES spectra of the undoped and doped ZnO films grown on the sapphire substrate compared to those of bulk ZnO single crystals. The arrows indicate a sub-peak located at the binding energy of 5 eV, where the binding energy is referred to the Fermi energy.

face. The heavily Al-doped films (n on the order of 10^{20} cm^{-3}) on the sapphire substrate showed a similar HX-PES profile of the bulk single crystal with the (0001) face, whereas the sub-peak at $E_B \approx 5$ eV was not clearly observed in the undoped and Ga- and In-doped films on the sapphire substrate. Note that the sub-peak at $E_B \approx 5$ eV was not observed in the lightly Al-doped (n on the order of 10^{19} cm^{-3}) films. The reason for the appearance of the sub-peak only on the (0001)-face is unclear at present, but this sub-peak can be used as a fingerprint to distinguish the polarity of the ZnO films.

We note that the intensity ratio between the O 1s and Zn 2p core-levels (I_{Zn}/I_O) in HX-PES varies with the surface polarity. When we normalized I_{Zn}/I_O to make it unity for a well-polished (000$\bar{1}$) face of ZnO single crystal, I_{Zn}/I_O of the (0001) face of the same single crystal was evaluated to be about 1.3. This relatively intense Zn 2p peak of the (0001) face was observed and could be reproduced for ZnO single crystals obtained from several different companies [32–34]. The difference in the I_{Zn}/I_O can be attributed to photoelectron-diffraction phenomena. In fact, such a difference in the intensity ratio has been reported for AlN, which has the same crystal structure as ZnO [35]. The intensity ratio between N 1s and Al 2p core-levels varies with the surface polarity of AlN owing to photoelectron-diffraction phenomena and is used for determining the crystalline polarity. Thus, I_{Zn}/I_O can be an indicator allowing polarity identification with HX-PES. The I_{Zn}/I_O of the films on the sapphire substrate was less than 1.2 for the undoped films and 1.3 or more for the heavily Al-doped ones. We note that the Ga-doped films deposited on the sapphire substrate have a multi-domain structure with a mixture of columnar grains with the (0001) and (000$\bar{1}$) faces, as determined from the CAICISS analyses. We obtained I_{Zn}/I_O of these Ga-doped films as 1.2, which was an intermediate value between that of the (0001) and (000$\bar{1}$) faces. Thus, we conclude that I_{Zn}/I_O is an appropriate indicator for assigning film polarity.

Table 2 summarizes the results of CBED, CAICISS, and HX-PES measurements in terms of the crystalline polarity. This table clearly shows that the presence of the sub-peak at $E_B = 5$ eV in the HX-PES spectra is an appropriate fingerprint for determining the crystalline polarity of ZnO. In fact, the sub-peak is clearly seen only for the film with the (0001) face, as evidenced by the CBED and CAICISS measurements. Table 2 also shows that I_{Zn}/I_O is another appropriate indicator for assessing the film polarity.

3.3. Polarity of ZnO films on glass substrates

Fig. 5 shows the valence band HX-PES spectra of the ZnO films grown on the glass substrate. The heavily Al-doped (n on the order of 10^{20} cm^{-3}) film on the glass substrate showed a similar spectral feature as the (0001) face of the ZnO single crystal, whereas the spectra of the undoped film on the glass substrate was similar to that of the (000$\bar{1}$) face for the ZnO single crystal. When we apply the appearance of the sub-peak as a fingerprint of the (0001) face, the polarity of the ZnO films on the glass substrate changed from the (000$\bar{1}$) face for the undoped film to the (0001) face for the heavily Al-doped film, similar to that observed for the ZnO films on the sapphire substrate. Moreover, I_{Zn}/I_O was larger than 1.31 for the heavily Al-doped film on the glass substrate, while it was 1.17 for the nominally undoped film grown on the glass substrate. $I_{Zn}/I_O < 1.2$ was obtained for the (000$\bar{1}$) face of single crystalline epitaxial films and $I_{Zn}/I_O > 1.3$ for the (0001) face. Thus, we conclude that the PLD-grown ZnO films on the SiO_2 glass substrate have the (0001) face when the films are prepared with the heavily Al-doped target by PLD. This result is important for understanding the polarity change of ZnO due to heavy Al-doping; we do not need to consider any special atomic arrangement at the ZnO/substrate interface for explaining the polarity change, because the polarity change of ZnO films by doping occurred regardless of the type of substrate used.

3.4. Polarity of a multilayer film

Finally, we discuss the results for a multilayer film with an [undoped ZnO]/[heavily Al-doped ZnO]/sapphire structure. Fig. 6 shows the CAICISS spectra obtained from the multilayer film with a few-monolayer-thick heavily Al-doped layer between the substrate and the undoped ZnO film. The CAICISS spectra measured for the top of the undoped ZnO layer was similar to that of the (000$\bar{1}$) surface of bulk ZnO, although heavily Al-doped films had the (0001) face when their

Table 2
Polarity of ZnO films grown on sapphire substrates determined using CAICISS, CBED, HX-PES spectra of the valence band region and the relative intensity ratio between O 1s and Zn 2p core levels (I_{Zn}/I_O).

ZnO film	Polarity [CAICISS]	Polarity [CBED]	Polarity [valence]	Polarity [I_{Zn}/I_O]
Undoped	(000$\bar{1}$)	(000$\bar{1}$)	(000$\bar{1}$)	(000$\bar{1}$)
0.1 mol% Al-doped	(000$\bar{1}$)	Not measured	(000$\bar{1}$)	(000$\bar{1}$)
1 mol% Al-doped	(0001)	(0001)	(0001)	(0001)
1 mol% Ga-doped	Mixture	Not measured	(000$\bar{1}$)	Mixture
1 mol% In-doped	Not measured	Not measured	(000$\bar{1}$)	Mixture

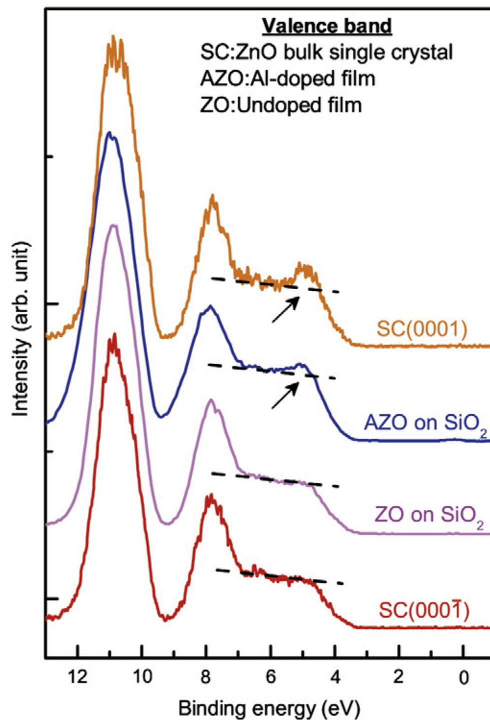

Fig. 5. HX-PES spectra of the undoped and doped ZnO films grown on SiO_2 glass substrates. Arrows indicates a sub-peak located at the binding energy of 5 eV.

thickness was a few hundred nanometers, as shown in Table 1. These results show that initiation of film deposition with the heavily Al-doped layer is not sufficient for the formation of ZnO nuclei with the (0001) face. That is, a heavily Al-doped buffer layer of a few monolayers is not effective for forming the (0001) face. Thus, a thickness greater than a few monolayers is required to grow ZnO films with the (0001) face.

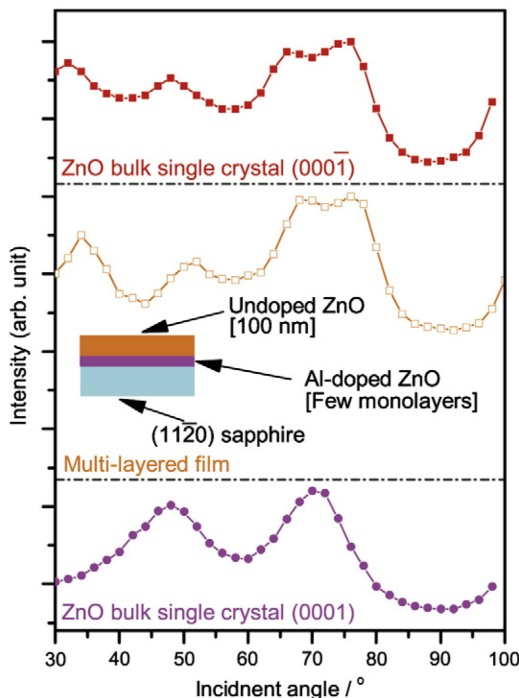

Fig. 6. CAICISS spectra for a multilayer film having the [undoped ZnO]/[heavily Al-doped ZnO]/sapphire structure. The inset shows a schematic diagram of the multilayer film.

4. Discussion

Since polarity change by heavy doping with Al was observed not only for the films deposited on a crystalline substrate (sapphire), but also on a non-crystalline substrate (silica glass), the polarity change observed in this study cannot be explained on the basis of heteroepitaxy, assuming alignment of the ZnO lattice on the atomic scale. Most polarity change phenomena reported in previous studies have been explained by assuming the matching of the oxygen or cation sublattice at the heterointerface. For example, the polarity inversion of ZnO by the insertion of MgO buffer layers is understood by assuming compatibility of the oxygen sublattice at the (0001) face of ZnO and the (111) face of MgO [13]. A macroscopic and phenomenological explanation has to be considered to explain the polarity change observed in this study because the polarity change due to heavy Al-doping occurred for both sapphire (crystalline) and glass (amorphous) substrates.

It is obvious that Al-doping results in a decrease in the grain size in the films both on sapphire and glass substrates, as shown in Fig. 1. Therefore, it could be considered that the grain size shrinkage affects the film polarity. However, the Ga- or In-doped films showed grain sizes as small as those in the Al-doped films, regardless of the fact that the films had the (000$\bar{1}$) face. This indicates that grain size reduction is not a critical factor for the film polarity.

The difference in vapor pressure of the elements under consideration is an issue for understanding the polarity change observed in this study. The vapor pressure of Zn is much higher than that of Al; therefore, there is a possibility that nucleation of Al-doped ZnO films with the (0001) face was initiated by condensation of Al at the nucleation stage. In fact, the re-evaporation of Zn during PLD growth of a ZnO-based alloy causes a deviation in the film composition from the target composition [36]. This assumption is consistent with the dopant dependence of the polarity change because Ga and In with relatively higher vapor pressure than Al could not induce a perfect polarity change. It should be noted that the insertion of heavily Al-doped buffer layers was not effective for the polarity inversion. This means that very small nuclei cannot initiate the growth of ZnO grains with the (0001) face. Even if condensation of Al is essential to change the polarity, this phenomenon cannot be explained by the adsorption of atomic-scale Al–O clusters or by few-atomic-layer-thick Al-rich layers. In fact, a TEM image shown in our previous report revealed the absence of an interfacial phase, such as Al_2ZnO_4 [18]. Thus, we can conclude that the polarity change is not simply due to the condensation of Al at the ZnO/substrate interface at the nucleation stage.

The polarity change was not significant in the Ga- and In-doped films. However, we should be careful in assuming that Ga and In are not appropriate for deposition of the (0001) films because the n of the In and Ga-doped films deposited in this study was relatively low compared to that of the heavily Al-doped films, as shown in Table 1. The experimental results suggest that there is a polarity change for films with a very high n, on the order of $10^{20}\,cm^{-3}$; however, it is difficult to state that the Al-doping causes the polarity change. Both the CAICISS and HX-PES spectra revealed that the Ga-doped and In-doped films had a multi-domain structure with a mixture of (0001) and (000$\bar{1}$) faces. To enable fair comparison between Al-, Ga-, and In-doped films, we need to optimize the growth conditions of the films with Ga- and In-doping to achieve very high electron concentrations.

5. Conclusions

We have shown that polarity inversion in ZnO thin films by Al-doping occurs not only on sapphire substrates, but also on SiO_2 glass substrates. We also demonstrated that HX-PES is a possible technique for determining the crystalline polarity of ZnO. Since an apparent polarity change due to Al-doping was observed at the ZnO/glass structure, the essential parameter governing the polarity of the film is unlikely to be lattice matching at the heterointerface between ZnO and the substrate,

rather phenomenological or macroscopic parameters, e.g., electron density in the ZnO nuclei or chemical composition of the nuclei first crystallized on the substrate surface, are more important than lattice compatibility at the ZnO/substrate interface.

From an engineering viewpoint, polarity-selective growth on non-crystalline substrates is a critical and desirable technology. Thus, our finding is likely favorable for engineers seeking a way to control the polarity of ZnO on non-crystalline substrates. However, the current experiments were carried out only with relatively high growth temperatures, which is not appropriate for low-temperature growth of ZnO on organic substrates for example. Thus, a more detailed mechanism to control polarity-selective growth of ZnO with relative low growth temperatures is essential for broader applications such as flat panel displays, touch screens, and organic LEDs.

Acknowledgments

This study was partly supported by a Grant in Aid for Construction of the World Premiere Research Institute (WPI) strategy promoted by the Ministry of Education, Culture, Sports, Science and Technology (MEXT), Japan. The HX-PES measurements were performed under the approval of the NIMS Beamline Station (Proposal Nos. 2007A4609, 2007B4607, 2008A4603, and 2009A4604). The authors are grateful to HiSOR, Hiroshima University, and JAEA/SPring-8 for the development of HX-PES at BL15XU of SPring-8. This study was also partially supported by a Grant-in-Aid for Scientific Research from the Japan Society for Promotion of Science, and MEXT, Japan. We also acknowledge the contributions of Mrs. Naoko Tateyama and Mrs. Hiroko Ishii for their administration.

References

[1] T. Minami, MRS Bull. 25 (2000) 38.
[2] T. Minami, Semicond. Sci. Technol. 20 (2005) S35.
[3] H. Ohta, K. Kawamura, M. Orita, M. Hirano, H. Sarukura, H. Hosono, Appl. Phys. Lett. 77 (2000) 475.
[4] A. Tsukazaki, A. Ohtomo, T. Onuma, M. Ohtani, T. Makino, M. Sumiya, K. Ohtani, S.F. Chichibu, S. Fuke, Y. Segawa, H. Ohno, H. Koinuma, M. Kawasaki, Nat. Mater. 4 (2005) 42.
[5] E.M.C. Fortunato, P.M.C. Barquinha, A.C.M.B.G. Pimentel, A.M.F. Goncalves, A.J.S. Marques, R.F.P. Martins, L.M.N. Pereira, Appl. Phys. Lett. 85 (2004) 2541.
[6] R.L. Hoffman, B.J. Norris, J.F. Wager, Appl. Phys. Lett. 82 (2003) 733.
[7] A. Wander, F. Schedin, P. Steadman, A. Norris, R. McGrath, T.S. Turner, G. Thornton, N.M. Harrison, Phys. Rev. Lett. 86 (2001) 3811.
[8] N. Ohashi, K. Takahashi, S. Hishita, I. Sakaguchi, H. Funakubo, H. Haneda, J. Electrochem. Soc. 154 (2007) D82.
[9] N. Ohashi, K. Kataoka, T. Ohgaki, I. Sakaguchi, H. Haneda, K. Kitamura, M. Fujimoto, Jpn. J. Appl. Phys. 46 (2007) L1042.
[10] H. Maki, I. Sakaguchi, N. Ohashi, S. Sekiguchi, H. Haneda, J. Tanaka, N. Ichinose, Jpn. J. Appl. Phys. 42 (2003) 75.
[11] H. Tampo, H. Shibata, K. Matsubara, A. Yamada, P. Fons, S. Niki, M. Yamagata, H. Kanie, Appl. Phys. Lett. 89 (2006) 132113.
[12] T. Ohnishi, A. Ohtomo, M. Kawasaki, K. Takahashi, M. Yoshimoto, H. Koinuma, Appl. Phys. Lett. 72 (1998) 824.
[13] H. Kato, K. Miyamoto, M. Sano, T. Yao, Appl. Phys. Lett. 84 (2004) 4562.
[14] Y. Wang, X.L. Du, Z.X. Mei, Z.Q. Zeng, M.J. Ying, H.T. Yuan, J.F. Jia, Q.K. Xue, Z. Zhang, Appl. Phys. Lett. 87 (2005) 051901.
[15] S.-K. Hong, T. Haneda, Y. Chen, H.-J. Ko, T. Yao, D. Imai, K. Araki, M. Shinohara, Appl. Surf. Sci. 190 (2002) 491.
[16] J.S. Park, S.K. Hong, T. Minegishi, S.H. Park, I.H. Im, T. Hanada, M.W. Cho, T. Yao, J.W. Lee, J.Y. Lee, Appl. Phys. Lett. 90 (2007) 201907.
[17] I. Ohkubo, A. Ohtomo, T. Ohnishi, Y. Mastumoto, H. Koinuma, M. Kawasaki, Surf. Sci. 443 (1999) 1043.
[18] Y. Adachi, N. Ohashi, T. Ohgaki, I. Sakaguchi, H. Haneda, T. Ohnishi, M. Lippmaa, J. Mater. Res. 23 (2008) 3269.
[19] S.K. Hong, T. Hanada, H.H. Ko, Y. Chen, T. Yao, D. Imai, K. Araki, M. Shinohara, K. Saitoh, M. Terauchi, Phys. Rev. B 65 (2002) 115331.
[20] J.S. Park, T. Minegishi, S.H. Lee, I.H. Im, S.H. Park, T. Hanada, T. Goto, M.W. Cho, S.K. Hong, J.H. Chang, J. Vac. Sci. Technol. A 26 (2008) 90.
[21] A.N. Mariano, R.E. Hanneman, J. Appl. Phys. 34 (1963) 384.
[22] H. Tampo, P. Fons, A. Yamada, K.K. Kim, H. Shibata, K. Matsubara, S. Niki, H. Yoshikawa, H. Kanie, Appl. Phys. Lett. 87 (2005) 141904.
[23] K. Kobayashi, M. Yabashi, Y. Takata, T. Tokushima, S. Shin, K. Tamasaku, D. Miwa, T. Ishikawa, H. Nohira, T. Hattori, Y. Sugita, O. Nakatsuka, A. Sakai, S. Zaima, Appl. Phys. Lett. 83 (2003) 1005.
[24] N. Ohashi, Y. Adachi, T. Ohsawa, K. Matsumoto, I. Sakaguchi, H. Haneda, S. Ueda, H. Yoshikawa, K. Kobayashi, Appl. Phys. Lett. 94 (2009) 122102.
[25] K. Nakahara, T. Tanabe, H. Takasu, P. Fons, K. Iwata, A. Yamada, K. Matsubara, R. Hunger, S. Niki, Jpn. J. Appl. Phys. 40 (2001) 250.
[26] H. Maki, N. Ichinose, S. Sekiguchi, N. Ohashi, T. Nishihara, H. Haneda, J. Tanaka, J. Jpn. J. Appl. Phys. 38 (1999) 2741.
[27] T. Mitate, S. Mizuno, H. Takahata, R. Kakegawa, T. Matsuoka, N. Kuwano, Appl. Phys. Lett. 86 (2005) 134103.
[28] T. Ohsawa, N. Ohashi, Y. Adachi, I. Sakaguchi, H. Ryoken, K. Matsumoto, H. Haneda, S. Ueda, H. Yoshikawa, K. Kobayashi, Appl. Phys. Lett. 92 (2008) 232108.
[29] T. Ohsawa, Y. Adachi, I. Sakaguchi, H. Ryoken, K. Matsumoto, H. Haneda, S. Ueda, H. Yoshikawa, K. Kobayashi, N. Ohashi, Chem. Mater. 21 (2009) 144.
[30] K. Kobayashi, Nucl. Inst. Meth. Phys. Res. A 601 (2009) 32.
[31] N. Ohashi, I. Sakaguchi, S. Hishita, Y. Adachi, H. Haneda, T. Ogino, J. Appl. Phys. 92 (2002) 2378.
[32] K. Maeda, M. Sato, I. Niikura, T. Fukuda, Semicond. Sci. Technol. 20 (2005) S49.
[33] D.C. Look, D.C. Reynolds, J.R. Sizelove, Solid State Commun. 105 (1998) 399.
[34] Tokyo Denpa Co., Ltd.
[35] V. Lebedev, B. Schröter, G. Kipshidze, W. Richter, J. Cryst. Growth 207 (1999) 266.
[36] H. Ryoken, N. Ohashi, I. Sakaguchi, Y. Adachi, S. Hishita, H. Haneda, J. Cryst. Growth 287 (2006) 134.